Decentralized policies for geometric pattern formation and path coverage

Marco Pavone and Emilio Frazzoli

Abstract

This paper presents a decentralized control policy for symmetric formations in multi-agent systems. It is shown that n agents, each one pursuing its leading neighbor along the line of sight rotated by a common offset angle α, eventually converge to a single point, a circle or a logarithmic spiral pattern, depending on the value of α. In the final part of the paper, we present a strategy to make the agents totally anonymous and we discuss a potential application to coverage path planning.

I. INTRODUCTION

The problem of prescribing to a multi-agent system a coordinated *global* behavior just relying on simple *local* rules is attracting an ever increasing interest. The potential advantages of employing decentralized (*i.e.* without a leader) teams of agents are in fact numerous. For instance, the intrinsic parallelism of a decentralized multi-agent system provides robustness to failures of single agents, and in many cases can guarantee better time efficiency. Moreover, it is possible to reduce the total implementation and operation cost, increase reactivity and system reliability, and add flexibility and modularity to monolithic approaches. Potential applications of multi-agent systems include search and rescue operations, humanitarian demining, manipulation in hazardous environments, planetary exploration, environmental monitoring and surveillance.

In this context, geometric pattern formation problems are currently of particular interest. Engineering applications include distributed sensing using mobile sensor networks, performing space missions with multiple spacecrafts, and automated parallel delivery of payloads. Moreover, geometric pattern formation problems are closely related to certain agreement problems. A rendez-vous implies agreement on a common origin, while a circle formation implies the agreement on both a common origin and a common unit distance (*i.e.*, the center and the radius of the circle); other examples can be found in [1]. Finally, decentralized algorithms for geometric pattern formations are also useful in modelling and understanding biological systems such as animal groups.

Recently, Justh and Krishnaprasad [2] presented a differential geometric setting for the problem of formation control and proposed two strategies to achieve, respectively, rectilinear and circle formation; their approach, however, requires all-to-all communication among agents. Jadbabaie *et al.* [3] formally proved that the nearest neighbor

This work was supported in part by the National Science Foundation, under grant no. CCR-0325716, and by the Air Force Office for Scientific Research, under contract no. F49620-02-1-0325. Any opinions, findings, and conclusions or recommendations expressed in this publication are those of the authors and do not necessarily reflect the views of the sponsoring agencies.

Marco Pavone and Emilio Frazzoli are with the Laboratory for Information and Decision Systems, Department of Aeronautics and Astronautics, Massachusetts Institute of Technology, Cambridge, MA 02139, {pavone, frazzoli}@mit.edu

algorithm by Vicsek [4] causes all agents to eventually move in the same direction, despite the absence of centralized coordination and despite the fact that each agent's set of nearest neighbors change with time as the system evolves. Jeanne *et al.* [5] and Paley *et al.* [6] studied the connections between phase models of coupled oscillators and kinematic models of groups of self-propelled particles and derived control laws for parallel motions and circular motions. Olfati-Saber and Murray [7] and Leonard *et al.* [8] used potential function theory to prescribe flocking behavior. Lin *et al.* [9] exploited cyclic pursuit to achieve alignment among agents, while Marshall *et al.* in [10] and in [11] extended the classic cyclic pursuit to a system of wheeled vehicles, each subject to a single non-holonomic constraint, and studied the possible equilibrium formations and their stability.

The contribution of this paper is three-fold. As a first contribution, we develop a distributed control policy that allows the robots to achieve different symmetric formations. The key features of the proposed approach are global stability and the possibility to achieve with the same simple control law different formations. Our approach is inspired by the cyclic pursuit strategy, where each agent i pursues the next $i+1$ (modulo n, where n is the number of agents) along the line of sight. It is well known that, under cyclic pursuit, the agents eventually converge to a single point (see, *e.g.*, [12]). Cyclic pursuit is an attractive approach since it is decentralized and requires the minimum number of communication links (n links for n agents) to achieve a formation.

Our control policy generalizes the notion of classic cyclic pursuit by letting each of the n mobile agents pursue its leading neighbor along the line of sight *rotated* by a common offset angle α.

We first assume, in Section III, that each agent is a simple integrator, *i.e.*, a dynamical system with no kinematic constraints on its motion. It is shown that our simple control policy can provide, depending on the value of α, rendez-vous to a point (thus generalizing the classic cyclic pursuit result that is obtained for $\alpha = 0$), evenly spaced circle formation and evenly spaced logarithmic spirals. These results are also illustrative of the intrinsic symmetry that characterizes cyclic pursuit. The study of the proposed control policy relies on an original *parametric* spectral analysis of some special types of circulant matrices.

Then, in Section IV, we extend the above linear scenario to one in which each agent is a non-holonomic mobile robot. The fact that we now consider differentially driven mobile robots complicates the coordination problem, due to the non-holonomic constraints. We address this problem by input-output feedback linearizing the system and by adapting the aforementioned control policy to the linearized input-output dynamics, represented by a double integrator system. The control of non-holonomic wheeled mobile robots by state feedback linearization was introduced in [13] and has been often exploited in the context of formation control, for example in [14]. The closed-loop behaviors are, depending on the value of α, *globally stable* rendez-vous to a point, *globally stable* evenly spaced circle formation and *globally stable* evenly spaced logarithmic spirals. In [11], a formation control law for non-holonomic wheeled robots in cyclic pursuit is introduced and elegantly studied. It is shown that, depending on the value of a gain, *locally stable* rendez-vous to a point, *locally stable* evenly spaced circle formation and *locally stable* evenly spaced logarithmic spirals are achieved. However, it turns out that these regular formations are not the only stable behaviors. Simulations, reported in [15], indicate that when the vehicles do not converge to a generalized regular polygon formation, they instead fall into a different kind of order: the vehicles "weave" in and out, while the formation as a whole moves along a linear trajectory. Therefore, our globally stable control policy may represent a significant improvement as far as potential applications are concerned.

As a second contribution, we propose, in section V, a strategy based on the concept of convex hull to make our algorithm anonymous. To the best of our knowledge, it is the first time that the anonymity issue is discussed in the context of cyclic pursuit. The idea is quite simple: each agent checks if it is on the convex hull of the set of all agents; if an agent happens to be a vertex of the convex hull, it pursues the agent on the next vertex of the convex hull, otherwise it performs a convex hull reaching strategy. In this way, the agents are made totally anonymous.

Finally, in Section VI, we discuss a practical problem where our generalized version of cyclic pursuit may be a suitable and advantageous approach; in particular, we consider the path planning problem, where the objective is to ensure that at least one agent eventually moves to within a given distance from any point in the target environment (see [16] for a complete survey on the problem). This problem can be efficiently solved by means of symmetric Archimedes spiral formations (spirals with the property that successive windings have a constant separation distance). We will show, without a detailed mathematical analysis, that it is possible to achieve an Archimedes spiral formation by making the offset angle α a function of locally available information. This case study also illustrates how in our framework it is possible to achieve more complicated symmetric formations.

II. Mathematical Background

In this section, we provide some definitions and results concerning the theory of circulant matrices, which will be later applied to analyze the proposed control strategy.

A. Circulant Matrices

A circulant matrix of order n is a square matrix of the form:

$$C = \begin{pmatrix} c_1 & c_2 & \dots & c_n \\ c_n & c_1 & \dots & c_{n-1} \\ \vdots & \vdots & & \vdots \\ c_2 & c_3 & \dots & c_1 \end{pmatrix}.$$

The elements of each row of C are identical to those of the previous row, but are shifted one position to the right and wrapped around. The whole circular matrix is evidently determined by the first row and we can write:

$$C = \mathrm{circ}[c_1, c_2, \dots, c_n].$$

A circulant matrix of order n is diagonalizable by the Fourier matrix (see [17] for details). Hence eigenvalues and eigenvectors of a circulant matrix C can be readily determined.

B. Block Circulant Matrices

Let $A_1, A_2, \ldots, A_n$ be square matrices each of order m. A *block circulant* matrix of type (m, n) is a matrix of order mn of the form:

$$\hat{A} = \begin{pmatrix} A_1 & A_2 & \ldots & A_n \\ A_n & A_1 & \ldots & A_{n-1} \\ \vdots & \vdots & & \vdots \\ A_2 & A_3 & \ldots & A_1 \end{pmatrix}.$$

Note that $\hat{A}$ is not necessarily circulant (only *block* circulant). The entire matrix is determined by the first block row and we can write:

$$\hat{A} = \mathrm{circ}[A_1, A_2, \ldots, A_n].$$

The Fourier matrix provide a diagonalization formula in the special case where all submatrices A_i are themselves circulant [17]. In the general case, a block circulant matrix can only be *block* diagonalized by means of the Fourier matrix (see [17] for details). Define $\varphi_i = e^{2(i-1)\pi j/n}$ where $j = \sqrt{-1}$; each diagonal block has the following structure:

$$D_i = A_1 + \varphi_i A_2 + \varphi_i^2 A_3 + \ldots + \varphi_i^{n-1} A_n, \qquad i = 1, 2, \ldots, n. \tag{1}$$

Since the eigenvalues of a block diagonal matrix are the collection of all the eigenvalues of each diagonal block, the block diagonalization formula greatly simplify the study of the eigenvalues of a block circulant matrix.

III. FORMATION CONTROL: HOLONOMIC ROBOTS

Consider in the plane n mobile agents (uniquely labelled by an integer $i \in 1, 2, \ldots, n$), where agent i pursues the next $i+1$, modulo n. Let $\boldsymbol{\xi}_i(t) = [x_i(t), y_i(t)]^T \in \mathbb{R}^2$ be the position at time $t \geq 0$ of the i^{th} agent, where $i \in 1, 2, \ldots, n$. The kinematics of each agent is described by a simple integrator:

$$\dot{\boldsymbol{\xi}}_i = \mathbf{u}_i. \tag{2}$$

In the classic cyclic pursuit strategy the control input is:

$$\mathbf{u}_i = k(\boldsymbol{\xi}_{i+1} - \boldsymbol{\xi}_i), \quad k \in \mathbb{R}^+. \tag{3}$$

Thus, agent i pursues its leading neighbor, agent $i+1$, along the line of sight, with a velocity proportional to the vector from agent i to agent $i+1$. The overall system dynamics is in compact form:

$$\dot{\boldsymbol{\xi}} = C\boldsymbol{\xi}, \tag{4}$$

where $\boldsymbol{\xi} = [\boldsymbol{\xi}_1^T, \boldsymbol{\xi}_2^T, \ldots, \boldsymbol{\xi}_n^T]^T$ and C is the circulant matrix $C = \mathrm{circ}[-1, 0, 1, 0, \ldots, 0]$. Hence, classic linear pursuit can be completely analyzed relying on the classic theory of circulant matrix.

Suppose, now, we extend the aforementioned classic linear cyclic pursuit scenario to one in which each agent pursues the leading neighbor along the line of sight *rotated* by a common offset angle $\alpha \in [-\pi, \quad \pi]$. Thus, the control input for each agent i is given by:

$$\mathbf{u}_i = kR(\alpha)(\boldsymbol{\xi}_{i+1} - \boldsymbol{\xi}_i), \tag{5}$$

where $R(\alpha)$ is the rotation matrix:

$$R(\alpha) = \begin{pmatrix} \cos\alpha & \sin\alpha \\ -\sin\alpha & \cos\alpha \end{pmatrix}.$$

The overall dynamics of the n agents is:

$$\dot{\boldsymbol{\xi}} = k\hat{A}\boldsymbol{\xi}, \tag{6}$$

where $\boldsymbol{\xi} = [\boldsymbol{\xi}_1^T, \boldsymbol{\xi}_2^T, \ldots, \boldsymbol{\xi}_n^T]^T$ and $\hat{A}$ is now the block circulant matrix $\hat{A} = \mathrm{circ}[-R(\alpha), R(\alpha), 0_{2\mathrm{x}2}, \ldots, 0_{2\mathrm{x}2}]$.

It is easy to see that the centroid of the agents is stationary. In the remainder of the paper, we will assume, without loss of generality, that $k = 1$.

In order to analyze the different geometric patterns achievable by system (6) for the various values of α, we start by studying the eigenvalues and eigenvectors of $\hat{A}$.

A. Eigenvalues of $\hat{A}$

Given the block diagonalization formula (1), the eigenvalues of $\hat{A}$ can be readily determined.

Theorem 3.1: The eigenvalues of $\hat{A}$ are the collection of:

$$\lambda_i^{\pm} = (\varphi_i - 1)e^{\pm j\alpha}, \tag{7}$$

for $i = 1, 2, \ldots, n$

Proof: As stated in the previous section, $\hat{A}$ is *block* diagonalized by means of the Fourier matrix and each diagonal block has the structure (1) with $A_1 = -R(\alpha)$, $A_2 = R(\alpha)$ and $A_i = 0_{2\mathrm{x}2}$ for $i = 3, 4, \ldots, n$:

$$D_i = -R(\alpha) + \varphi_i R(\alpha), \qquad i = 1, 2, \ldots, n. \tag{8}$$

The characteristic polynomial of D_i is:

$$p_{D_i}(\lambda) = \lambda^2 - 2\lambda\cos\alpha(\varphi_i - 1) + (\varphi_i - 1)^2.$$

Therefore, we get:

$$\lambda_i^{\pm} = \cos\alpha(\varphi_i - 1) \pm \sqrt{(\cos^2\alpha - 1)(\varphi_i - 1)^2}.$$

Thus we obtain $\lambda_i^{\pm} = (\varphi_i - 1)e^{\pm j\alpha}$. Since the eigenvalues of a block diagonal matrix are the collection of all the eigenvalues of each diagonal block, we get the claim. ■

B. Analysis of the Eigenvalues of $\hat{A}$

The eigenvalues of $\hat{A}$ show the following property.

Lemma 3.1:

$$\lambda_i^+ = \overline{\lambda_{n-i+2}^-} \quad i = 2, 3, \dots, n. \tag{9}$$

Proof: The proof is straightforward:

$$\overline{\lambda_{n-i+2}^-} = \overline{(\varphi_{n-i+2} - 1)e^{-j\alpha}} = (\overline{\varphi_{n-i+2}} - 1)e^{j\alpha} =$$
$$= (e^{2\pi j[(i-1)-n]/n} - 1)e^{j\alpha} = (e^{2\pi j(i-1)} - 1)e^{j\alpha} = \lambda_i^+.$$

■

Define the set:

$$\mathcal{H} = \{\lambda_i^\pm, \quad i = 1, 2, \dots, n\}. \tag{10}$$

Let us now be more explicit with the structure of the eigenvalues; define:

$$\theta_i^\pm = \left(\frac{i-1}{n}\pi \pm \alpha\right). \tag{11}$$

After some algebraic manipulations we can write the eigenvalues $\lambda_i^\pm$ as:

$$\lambda_i^\pm = 2\sin\left(\frac{i-1}{n}\pi\right)(-\sin\theta_i^\pm + j\cos\theta_i^\pm). \tag{12}$$

Lemma 3.2: The block circulant matrix $\hat{A}$ has a zero eigenvalue with algebraic multiplicity $m_{\lambda=0} = 2$; the two zero-eigenvalues in $\mathcal{H}$ are $\lambda_1^\pm$.

Proof: If $i = 1$ clearly $\lambda_1^\pm = 0 \quad \forall\alpha$. If $i > 1$ it must be $\|\lambda_i^\pm\| \neq 0$ since the functions $\sin(\cdot)$ and $\cos(\cdot)$ can not be zero at the same time. ■

Lemma 3.3: The eigenvalues of $\hat{A}$ can have algebraic multiplicity at most $m_\lambda = 2$. In particular the non zero-eigenvalues that can separately collapse are $(\lambda_i^+, \lambda_i^-)$, $(\lambda_i^+, \lambda_{n-(i-2)}^-)$, $(\lambda_{n-(i-2)}^+, \lambda_i^-)$ and $(\lambda_{n-(i-2)}^+, \lambda_{n-(i-2)}^-)$ $i = 2, 3, \dots, n$.

Proof: The statement is true for the zero eigenvalue, obtained for $i = 1$. Consider therefore $i > 1$. As evident from equation (12), as α is varied, the eigenvalues move on circles with radius $r_i = 2\sin(\pi(i-1)/n)$; clearly, only the eigenvalues that move on the same circles can collapse. Since:

$$0 < \frac{i-1}{n}\pi < \pi \quad i = 2, 3, \dots, n,$$

for symmetry we deduce that the eigenvalues that move on the same circle are:

$$\lambda_i^+ \quad \lambda_{n-(i-2)}^+ \quad \lambda_i^- \quad \lambda_{n-(i-2)}^-, \quad i = 2, 3, \dots, n;$$

in fact, $\sin\left(\pi\frac{(n-(i-2))-1}{n}\right) = \sin\left(\pi\frac{i-1}{n}\right)$. Therefore just 4 eigenvalues move on the same circle (2 in the case that n is even and $i = n/2 + 1$; in particular these eigenvalues move on the most external circle since the argument of $\sin(\cdot)$ is $\pi/2$).

As it can be inferred from (12), as α is increased, the eigenvalues λ_i^+ and $\lambda_{n-(i-2)}^+$ move counter-clockwise with fixed phase difference $\delta = \pi(n - 2i + 2)/n$, while the eigenvalues λ_i^- and $\lambda_{n-(i-2)}^-$ move clockwise with the same fixed phase difference δ. Therefore at most two eigenvalues can collapse, in particular the eigenvalue λ_i^+ can collapse with the eigenvalues λ_i^- or $\lambda_{n-(i-2)}^-$; similarly for the other eigenvalues. ■

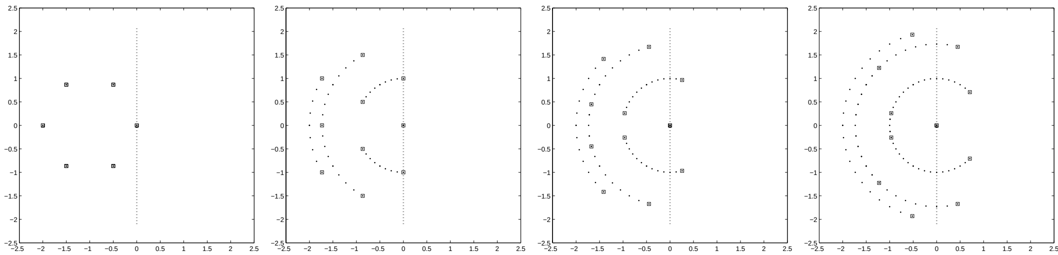

(a) $\alpha = 0$ (b) $\alpha = \pi/6$ (c) $\alpha = \pi/6 + \pi/12$ (d) $\alpha = 2\pi/6 + \pi/12$

Fig. 1. Eigenvalue placement for various α and $n = 6$. On the most external circle there are just two eigenvalues.

In the classic cyclic pursuit we have $\alpha = 0$; in this case it is straightforward to notice that the $2n-2$ non-zero eigenvalues in $\mathcal{H}$ lie in the open left half complex plane. Let us now consider the case $\alpha \neq 0$.

Theorem 3.2: Suppose:

$$k\pi/n < |\alpha| \leq (k+1)\pi/n, \tag{13}$$

where $k \in \mathbb{N}^0, \quad 0 \leq k \leq n-1$. The following statements hold:

(i) among the $2n-2$ non-zero eigenvalues $\in \mathcal{H}$, $2k$ eigenvalues lie in the open right half complex plane;

(ii) among the $2n-2$ non-zero eigenvalues $\in \mathcal{H}$, two eigenvalues lies on the imaginary axis if $|\alpha| = (k+1)\pi/n$ with $k = 0, 1, \ldots, n-2$.

Proof: Consider the case $\alpha \in]0, \quad \pi]$; the proof with $\alpha \in [-\pi, \quad 0[$ is analogous. Let us prove fact (i). From the previous considerations, the non-zero eigenvalues are obtained for $i > 1$. Let us firstly consider λ_i^-. Since $i > 1$ we have:

$$-\pi < \theta_i^- < \pi(n-1)/n \quad i = 2, 3, \ldots, n. \tag{14}$$

Therefore, we can just compare θ_i^- with zero to check for which indices i the condition $\sin(\theta_i^-) < 0$ holds.

For α chosen as in (13), θ_i^- is negative for $i = 2, 3, \ldots, k+1$, while for $i = k+2, k+3, \ldots, n$ we have that $\theta_i^- \geq 0$. Therefore, we can conclude that exactly k eigenvalues among the λ_i^- eigenvalues lie in the open right half complex plane. With similar arguments (or recalling Lemma 3.1) we can state that also k eigenvalues among the λ_i^+ eigenvalues lie in the open right half complex plane.

Next we consider statement (ii). From (14), a non-zero eigenvalue among the λ_i^- eigenvalues lies on the imaginary axis if and only if $\theta_i^- = 0$: this happens if $\alpha = (i-1)\pi/n$ for some $i = 2, 3, \ldots, n$, *i.e.* if $\alpha = (k+1)\pi/n$ with $k = 0, 1, \ldots, n-2$. The proof is completed considering Lemma 3.1. ■

C. Eigenvectors of $\hat{A}$

To study the possible polygons of pursuit, we have to study the eigenvectors of $\hat{A}$. Following [18], consider a compound vector of the form:

$$\mathbf{w} = [\mathbf{v}, \varphi\mathbf{v}, \ldots, \varphi^{n-1}\mathbf{v}]^T, \tag{15}$$

where $\mathbf{v}$ is a non-null 2-vector and φ is any n^{th} root of unity.

The vector $\mathbf{w}$ is an eigenvector of $\hat{A}$ with eigenvalue λ if and only if:

$$\hat{A}\mathbf{w} = \lambda\mathbf{w}. \tag{16}$$

The first few of the n compound rows of this equation are:

$$\begin{aligned}
(A_1 \quad + \varphi A_2 + \varphi^2 A_3 + \ldots + \varphi^{n-1} A_n \quad)\mathbf{v} &= \quad \lambda\mathbf{v}, \\
(A_n \quad + \varphi A_1 + \varphi^2 A_2 + \ldots + \varphi^{n-1} A_{n-1})\mathbf{v} &= \varphi\ \lambda\mathbf{v}, \\
(A_{n-1} + \varphi A_n + \varphi^2 A_1 + \ldots + \varphi^{n-1} A_{n-2})\mathbf{v} &= \varphi^2\lambda\mathbf{v}.
\end{aligned} \tag{17}$$

Each of the n compound rows in (17) reduces to the first compound row, and that can be rewritten as the eigenvector equation:

$$D\mathbf{v} = \lambda\mathbf{v}, \tag{18}$$

where the square matrix D of order 2 is:

$$D = A_1 + \varphi A_2 + \varphi^2 A_3 + \ldots + \varphi^{n-1} A_n. \tag{19}$$

The n eigenvector equations (18), for the n values of φ, are equivalent to the single eigenvector equation (16). In our case the i^{th} eigenvector equation is:

$$D_i\mathbf{v} = \lambda\mathbf{v}, \tag{20}$$

where:

$$D_i = -R(\alpha) + \varphi_i R(\alpha). \tag{21}$$

Note that the D_i matrices are exactly the diagonal blocks (8) computed before. We already know that the eigenvalues of D_i are $\lambda_i^{\pm} = (\varphi_i - 1)e^{\pm j\alpha}$. The i^{th} eigenvector equation for $\lambda_i^{\pm}$ becomes:

$$(\varphi_i - 1)\sin\alpha \begin{pmatrix} \mp j & 1 \\ -1 & \mp j \end{pmatrix} \mathbf{v} = \mathbf{0}.$$

Thus we get:

$$\mathbf{v} = \begin{pmatrix} 1 \\ \pm j \end{pmatrix}. \tag{22}$$

Theorem 3.3: The eigenvectors corresponding, respectively, to the eigenvalues λ_i^+ and λ_i^- are:

$$\begin{aligned}
\mathbf{w}_i^+ &= \left[1, j, \varphi_i, j\varphi_i, \ldots, \varphi_i^{(n-1)}, j\varphi_i^{(n-1)}\right]^T, \\
\mathbf{w}_i^- &= \left[1, -j, \varphi_i, -j\varphi_i, \ldots, \varphi_i^{(n-1)}, -j\varphi_i^{(n-1)}\right]^T.
\end{aligned} \tag{23}$$

Proof: Let us just make a direct verification. Consider firstly $\mathbf{w}_i^+$ and write shortly $\mathbf{w}_i^+ = \mathbf{w}$ and $\lambda_i^+ = \lambda$. Let us partition $\mathbf{w} \in \mathbb{C}^{2n}$ into n components $\chi := [\mathbf{w}_1, \mathbf{w}_2, \dots, \mathbf{w}_n]$. Expanding (16) for each component $\mathbf{w}_k$ we get:

$$-R(\alpha)\mathbf{w}_k + R(\alpha)\mathbf{w}_{k+1} = \lambda \mathbf{w}_k.$$

Further expanding, we obtain the identity:

$$\begin{pmatrix} -e^{j\alpha}\varphi_i^{(k-1)} + e^{j\alpha}\varphi_i^k \\ -je^{j\alpha}\varphi_i^{(k-1)} + je^{j\alpha}\varphi_i^k \end{pmatrix} = (\varphi_i - 1)\, e^{j\alpha} \begin{pmatrix} \varphi_i^{(k-1)} \\ j\varphi_i^{(k-1)} \end{pmatrix}.$$

The proof for $\mathbf{w}_i^-$ is analogous. ■

Remark 3.1: The eigenvectors of $\hat{A}$ do not depend on the offset angle α.

D. Independency of the eigenvectors of $\hat{A}$

An important question to be addressed is if $\hat{A}$ is defective for some α.

Lemma 3.4: Two eigenvectors $\mathbf{w}_p^+$ and $\mathbf{w}_q^-$ are linearly independent $\forall p, q \in \{1, 2, \dots, n\}$.

Proof: It is sufficient to observe the first two components of each eigenvector. ■

Theorem 3.4: The block circulant matrix $\hat{A}$ is diagonalizable $\forall \alpha \in [-\pi, \quad \pi]$.

Proof: From Theorem 3.2, an eigenvalue of $\hat{A}$ can have at most algebraic multiplicity $m_\lambda = 2$. In particular the couples that can collapse, beside the eigenvalues $\lambda_1^\pm$, are: (λ_i^+, λ_i^-), (λ_i^+, $\lambda_{n-(i-2)}^-$), ($\lambda_{n-(i-2)}^+$, λ_i^-) and ($\lambda_{n-(i-2)}^+$, $\lambda_{n-(i-2)}^-$) with $i = 2, 3, \dots, n$. A consequence of Lemma 3.4 is that the corresponding eigenvectors are linearly independent. The other eigenvectors are independent for the eigenspace independence theorem. Therefore the matrix $\hat{A}$ is diagonalizable. ■

E. Pattern formation

We are now ready to show the achievable geometric patterns. Since the block circulant matrix $\hat{A}$ is diagonalizable, the general solution has the form:

$$\boldsymbol{\xi}(t) = \sum_{k=1}^{q} \sum_{j=1}^{m_{\lambda_k}} \alpha_{kj} e^{t\lambda_k} \mathbf{w}_{kj}, \tag{24}$$

where q is the number of distinct eigenvalues, the α_{kj} are constants and the $\mathbf{w}_{kj}$ are the eigenvectors corresponding to the k^{th} eigenvalue.

We can rewrite (24) by picking out the two eigenvectors corresponding to the zero eigenvalues $\lambda_1^\pm$, *i.e.* $\mathbf{w}_1^\pm$, and replacing them with the two eigenvectors:

$$\mathbf{w}_G^1 = \frac{1}{2}\left(\mathbf{w}_1^+ + \mathbf{w}_1^-\right) = [1, 0, 1, 0, \dots, 1, 0],$$
$$\mathbf{w}_G^2 = \frac{1}{2j}\left(\mathbf{w}_1^+ - \mathbf{w}_1^-\right) = [0, 1, 0, 1, \dots, 0, 1],$$

eq. (24) becomes:

$$\boldsymbol{\xi}(t) = \sum_{k=2}^{q} \sum_{j=1}^{m_{\lambda_k}} \alpha_{kj} e^{t\lambda_k} \mathbf{w}_{kj} + x_G \mathbf{w}_G^1 + y_G \mathbf{w}_G^2, \tag{25}$$

where x_G and y_G are the coordinates of the center of mass. We are now ready to show how different geometric patterns can be achieved by modulating the angle α.

1) Rendez-vous to a point: Consider $|\alpha| < \pi/n$; from Theorem 3.2, all the non-zero eigenvalues lie in the open left half complex plane. Therefore we have:

$$\lim_{t \to +\infty} \boldsymbol{\xi}(t) = x_G \mathbf{w}_G^1 + y_G \mathbf{w}_G^2.$$

Therefore, for any initial condition, all agents exponentially converge to a single limit point: their initial center of mass. This result extends the classic cyclic pursuit result that is obtained when $\alpha = 0$.

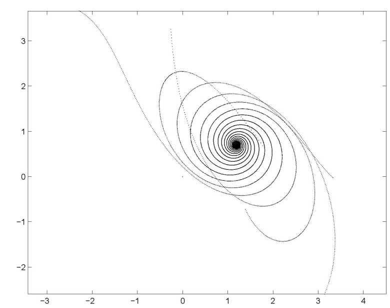

Fig. 2. *Rendez-vous* to a point for $n = 6$ agents and $\alpha = \pi/6 - \pi/12$.

2) Evenly spaced circle formation: Let us consider $\alpha = \pi/n$. From Theorem 3.2, besides the two zero eigenvalues, there are two non-zero eigenvalues lying on the imaginary axis, while all the other eigenvalues lie in the open left half complex plane. The imaginary eigenvalues are λ_n^+ and λ_2^- and are equal to $\mp j 2 \sin(\pi/n) = \mp j\gamma$.

We can rewrite (25) by picking out also the two eigenvectors corresponding to the imaginary eigenvalues, *i.e.* $\mathbf{w}_n^+$ and $\mathbf{w}_2^-$:

$$\boldsymbol{\xi}(t) = \sum_{k=4}^{q} \sum_{j=1}^{m_{\lambda_k}} \alpha_{kj} e^{t\lambda_k} \mathbf{w}_{kj} + d_1 e^{-jt\gamma} \mathbf{w}_n^+ + d_2 e^{jt\gamma} \mathbf{w}_2^- + x_G v_G^1 + y_G v_G^2, \tag{26}$$

where d_1 and d_2 are two constants. We replace the two complex eigenfunctions with two real independent eigenfunctions obtained as follows:

$$\mathbf{w}_{\text{dom}}^1 = \frac{1}{2} \left(e^{jt\gamma} \mathbf{w}_2^- + e^{-jt\gamma} \mathbf{w}_n^+ \right),$$
$$\mathbf{w}_{\text{dom}}^2 = \frac{1}{2j} \left(e^{jt\gamma} \mathbf{w}_2^- - e^{-jt\gamma} \mathbf{w}_n^+ \right).$$

Thus we get, defining $\delta_i = \frac{2\pi(i-1)}{n} \quad i = 1, 2, \ldots, n$:

$$\mathbf{w}_{\text{dom}}^1 = [\cos(\delta_1 + \gamma t), \sin(\delta_1 + \gamma t), \ldots, \cos(\delta_n + \gamma t), \sin(\delta_n + \gamma t)]^T,$$
$$\mathbf{w}_{\text{dom}}^2 = [\sin(\delta_1 + \gamma t), -\cos(\delta_1 + \gamma t), \ldots, \sin(\delta_n + \gamma t), -\cos(\delta_n + \gamma t)]^T.$$

We have for $t \to +\infty$:

$$\boldsymbol{\xi}(t) = c_1 \mathbf{w}_{\text{dom}}^1 + c_2 \mathbf{w}_{\text{dom}}^2 + x_G v_G^1 + y_G v_G^2.$$

Therefore, after a transient, the trajectory of each agent is (assuming $c_1 \neq 0$ and $c_2 \neq 0$):

$$x_i(t) \simeq c_1 \cos(\delta_i + \gamma t) + c_2 \sin(\delta_i + \gamma t) + x_G,$$

$$y_i(t) \simeq c_1 \sin(\delta_i + \gamma t) - c_2 \cos(\delta_i + \gamma t) + y_G,$$

i.e. a circular motion with center (x_G, y_G), radius $r = \sqrt{c_1^2 + c_2^2}$ and period $2\pi/\gamma$. The agents are evenly spaced since the angular distance between agent i and agent $i+1$ is $2\pi/n$.

If we take $\alpha = -\pi/n$, we have again, asymptotically, a circular motion, but the direction of motion is reversed.

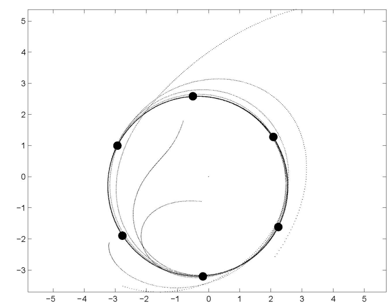

Fig. 3. Circle formation for $n = 6$ agents ($\alpha = \pi/6$).

3) Evenly spaced logarithmic spiral formation: Let us consider $\alpha \in]\pi/n, \quad 2\pi/n[$. From Theorem 3.2, besides the two zero eigenvalues, there are two complex positive eigenvalues: λ_n^+ and λ_2^- equal, shortly, to $\beta \mp j\gamma$. Therefore, with similar arguments, we obtain that the trajectory of each agent is for t quite large (assuming $c_1 \neq 0$ and $c_2 \neq 0$):

$$x_i(t) \simeq e^{\beta t} \left(c_1 \cos(\delta_i + \gamma t) + c_2 \sin(\delta_i + \gamma t)\right) + x_G,$$

$$y_i(t) \simeq e^{\beta t} \left(c_1 \sin(\delta_i + \gamma t) - c_2 \cos(\delta_i + \gamma t)\right) + y_G,$$

i.e. a logarithmic spiral with growing rate β. The agents are evenly spaced since the angular distance between agent i and agent $i+1$ is $2\pi/n$.

If we take $\alpha \in]-2\pi/n, \quad -\pi/n[$, we have, asymptotically, the same pattern, except that the direction of motion is reversed.

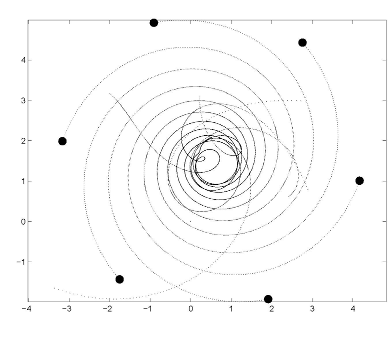

Fig. 4. Spiral formation for $n = 6$ agents and $\alpha = \pi/6 + \pi/12$.

IV. FORMATION CONTROL: NON-HOLONOMIC ROBOTS

We now extend the previous formation control law to the non-holonomic case. Consider, for instance, that each agent is a Hilare-type mobile robot with nonlinear state model [14]:

$$\begin{pmatrix} \dot{x}_i \\ \dot{y}_i \\ \dot{\theta}_i \\ \dot{v}_i \\ \dot{\omega}_i \end{pmatrix} = \begin{pmatrix} v_i \cos\theta_i \\ v_i \sin\theta_i \\ \omega_i \\ 0 \\ 0 \end{pmatrix} + \begin{pmatrix} 0 & 0 \\ 0 & 0 \\ 0 & 0 \\ 1/m & 0 \\ 0 & 1/J \end{pmatrix} \begin{pmatrix} F_i \\ \tau_i \end{pmatrix}, \qquad (27)$$

where $r_i = (x_i, y_i)^T$ is the inertial position of the i^{th} robot, θ_i is the orientation, v_i is the linear speed, ω_i is the angular speed, m is the mass, J is the moment of inertia, F_i is the force input and τ_i is the torque input. Let $\boldsymbol{u}_i = (F_i, \tau_i)^T$. In the model it is evident the non-holonomic Pfaffian constraint: $\dot{x}_i \sin\theta_i - \dot{y}_i \cos\theta_i = 0$. Assume that we want to maintain in formation a point off the wheel axis of the agents. Specifically, let us define, as in [14], the "hand" position of an agent to be the point $h = (h_x, h_y)$ that lies a distance $L \neq 0$ along the line that is normal to the wheel axis and intersects the wheel axis at the center point, as shown in Fig. 5. It is possible to show [14] that a Hilare-type robot can be feedback linearized about the hand position, the diffeomorphism that transforms the system in normal form is *globally* invertible and the corresponding zero dynamics are *stable*. Since we can reasonably consider sensors located at the hand, this approach does not indeed represent a significant limitation.

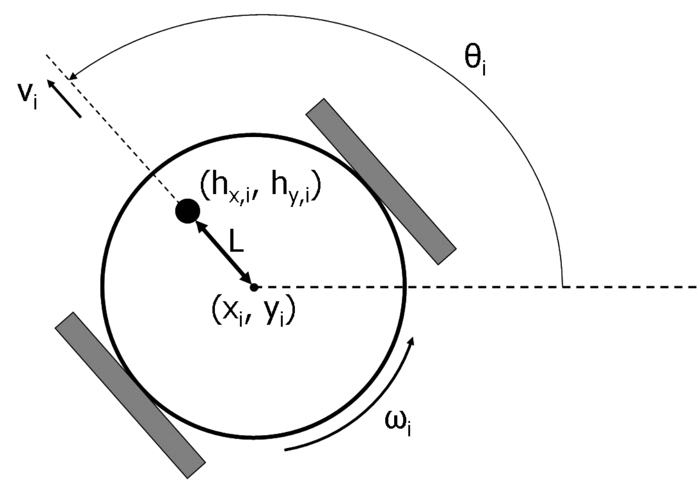

Fig. 5. Nonholonomic differentially driven mobile robot (adapted from [14]).

The hand position dynamics is given by $\ddot{\mathbf{h}}_i = \boldsymbol{\nu}_i$ and the output feedback linearizing control is given by:

$$\mathbf{u}_i = \begin{pmatrix} \frac{1}{m}\cos\theta_i & -\frac{L}{J}\sin\theta_i \\ \frac{1}{m}\sin\theta_i & \frac{L}{J}\cos\theta_i \end{pmatrix}^{-1} \times \left[\boldsymbol{\nu}_i - \begin{pmatrix} -v_i\omega_i \sin\theta_i - L\omega_i^2 \cos\theta_i \\ v_i\omega_i \cos\theta_i - L\omega_i^2 \sin\theta_i \end{pmatrix} \right]. \qquad (28)$$

Let us focus, therefore, on the control law for the hand position. To have stable circle and spiral formations, the hand position velocity should be as in Eq. (5). Thus, a possible approach is to consider a velocity tracking problem.

Let $\mathbf{v}_i = \dot{\mathbf{h}}_i$ and $\mathbf{v}_i^d = R(\alpha)(\mathbf{h}_{i+1} - \mathbf{h}_i)$ be the velocity and the desired velocity of the hand position, respectively. If we choose:

$$\boldsymbol{\nu}_i = -K\mathbf{v}_i + \mathbf{r}_i,$$

we get the first order system:

$$\dot{\mathbf{v}}_i + K\mathbf{v}_i = \mathbf{r}_i.$$

Choose now:

$$\mathbf{r}_i = \dot{\mathbf{v}}_i^d + K\mathbf{v}_i^d = R(\alpha)(\dot{\mathbf{h}}_{i+1} - \dot{\mathbf{h}}_i) + KR(\alpha)(\mathbf{h}_{i+1} - \mathbf{h}_i),$$

we obtain the following homogeneous first order differential equation:

$$\dot{\widetilde{\mathbf{v}}}_i + K\widetilde{\mathbf{v}}_i = \mathbf{0}, \tag{29}$$

where $\widetilde{\mathbf{v}}_i = \mathbf{v}_i - \mathbf{v}_i^d$. Eq. (29) describes the dynamics of the velocity error. If K is positive definite, the error dynamics is asymptotically stable.

Thus, the following control law applied to the hand position:

$$\boldsymbol{\nu}_i = K\left(R(\alpha)(\mathbf{h}_{i+1} - \mathbf{h}_i) - \dot{\mathbf{h}}_i\right) + R(\alpha)(\dot{\mathbf{h}}_{i+1} - \dot{\mathbf{h}}_i), \tag{30}$$

where K is positive definite, asymptotically provides the desired hand velocity. This implies that control law (30), together with (28), guarantees, depending on the value of α, *globally stable* rendez-vous to a point, *globally stable* evenly spaced circle formation and *globally stable* evenly spaced logarithmic spirals.

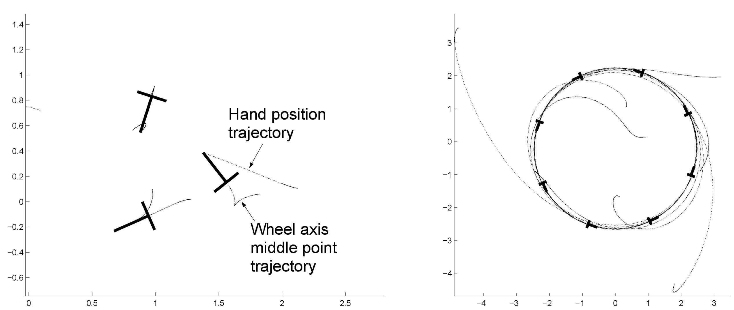

(a) Circle formation for $n = 8$ non-holonomic agents - detail

(b) Circle formation for $n = 8$ non-holonomic agents

Fig. 6. Formations of $n = 8$ non-holonomic agents.

Remark 4.1: The proposed control policy requires that each robot knows its orientation θ_i, its velocity $\dot{\mathbf{h}}_i$, the relative position $(\mathbf{h}_{i+1} - \mathbf{h}_i)$, the relative velocity $(\dot{\mathbf{h}}_{i+1} - \dot{\mathbf{h}}_i)$ and the total number of agents n. Note that agents do not recall past actions and observations (*i.e.*, they are oblivious). Oblivious algorithms are, by definition, self-stabilizing in the sense that they achieve their goal even in the presence of a finite number of sensor and control errors [1]. Moreover, no agent has to measure the absolute positions of other agents or its own. Communication among agents is needed only to exchange the identifier information.

Remark 4.2: It is interesting to compare our control policy with the control policy, similar in spirit, proposed by Marshall and coauthors in [11]. Marshall's approach can be summarized as follows. Consider a kinematic version of the dynamic model (27):

$$\begin{pmatrix} \dot{x}_i \\ \dot{y}_i \\ \dot{\theta}_i \end{pmatrix} = \begin{pmatrix} \cos\theta_i & 0 \\ \sin\theta_i & 0 \\ 0 & 1 \end{pmatrix} \begin{pmatrix} v_i \\ \omega_i \end{pmatrix}. \tag{31}$$

Let r_i denote the distance between unicycles numbered i and $i+1$, and let α_i be the angle from the i^{th} unicycle's heading to the heading that would take it directly towards unicycle $i+1$. The control law they consider is to assign unicycle i's linear speed v_i in proportion to r_i, while assigning its angular speed ω_i in proportion to α_i, that is:

$$v_i = k_r r_i \quad \text{and} \quad \omega_i = k_\alpha \alpha_i. \tag{32}$$

It is shown that, depending on the value of the ratio k_r/k_α and the total number of agents n, *locally stable* rendezvous to a point, *locally stable* evenly spaced circle formation and *locally stable* evenly spaced logarithmic spirals are achieved. However, it turns out that these regular formations are not the only stable behaviors. Simulations, reported in [15], indicate that when the vehicles do not converge to a generalized regular polygon formation, they instead fall into a different kind of order: the vehicles "weave" in and out, while the formation as a whole moves along a linear trajectory [15]. Therefore, our globally stable control policy may represent a significant improvement, as far as applications are concerned. Moreover, since we consider a dynamic model, the physical implementation is simplified.

V. Anonymous approach

In [1], an anonymous control policy for a team of agents is defined as follows:

1) all agents use the same algorithm for determining the next position;
2) agents cannot be distinguished by their appearances;
3) agents do not know their identifiers.

Clearly, the critical point in the classic cyclic pursuit approach is (3), since each robot does need to know its own identifier and the identifier of each other robot.

In order to overcome this problem, consider the following strategy, based on the concept of convex hulls (the convex hull of a set of points is the smallest convex set that contains the points). Each agent checks if it is on the convex hull of the set of all agents; if an agent happens to be a vertex of the convex hull, it pursues the agent on the next vertex (as determined by a common direction for the z axis, that we assume available to each agent) of the convex hull, otherwise it performs a convex hull reaching strategy. Uniqueness is the fundamental advantage of convex hull. We have considered a very simple convex hull reaching strategy: if an agent is not on the convex hull, it keeps moving along the current direction; at the beginning, a random direction is chosen.

A natural question that arises is: will an agent on the convex hull stay on the convex hull forever? To answer this question, consider, in the holonomic scenario, the change of coordinates:

$$\widetilde{\boldsymbol{\xi}_i} = \boldsymbol{\xi}_{i+1} - \boldsymbol{\xi}_i.$$

The trajectories of these difference vectors evolve according to the equation:

$$\dot{\widetilde{\boldsymbol{\xi}}}_i = R(\alpha)(\widetilde{\boldsymbol{\xi}}_{i+1} - \widetilde{\boldsymbol{\xi}}_i).$$

Clearly, the centroid in the new coordinates is fixed as well. In polar coordinates we get, after some manipulations, the system of equations:

$$\begin{aligned} \dot{\rho}_i = &\quad \rho_{i+1}\cos(\theta_{i+1} - \theta_i - \alpha) - \rho_i \cos\alpha, \\ \dot{\theta}_i = &\quad \tfrac{\rho_{i+1}}{\rho_i}\sin(\theta_{i+1} - \theta_i - \alpha) + \sin\alpha. \end{aligned} \tag{33}$$

A convex polygon of pursuit becomes concave when $\phi_{i+1} \doteq \theta_{i+1} - \theta_i$ becomes negative; ϕ_{i+1} evolves according to the equation:

$$\dot{\phi}_{i+1} = \frac{\rho_{i+2}}{\rho_{i+1}}\sin(\phi_{i+2} - \alpha) - \frac{\rho_{i+1}}{\rho_i}\sin(\phi_{i+1} - \alpha). \tag{34}$$

If $\phi_{i+1} = 0$, its time derivative is:

$$\dot{\phi}_{i+1} = \frac{\rho_{i+2}}{\rho_{i+1}}\sin(\phi_{i+2} - \alpha) + \frac{\rho_{i+1}}{\rho_i}\sin(\alpha). \tag{35}$$

It order to study the sign of $\dot{\phi}_{i+1}$, note that:

1) $0 \le \phi_{i+2} \le \pi$, otherwise agent $i+2$ would not be on the convex hull;
2) $\alpha \in [0 \quad 2\pi/n[$ as discussed in Section III.

Therefore, it is obvious from Eq. (35) that, when $\phi_{i+1} = 0$, $\dot{\phi}_{i+1}$ *can* be negative (unless $\alpha = 0$) and, thus, if $\alpha \neq 0$, an agent on the convex hull can leave the convex hull (in details, if ϕ_{i+1} becomes negative the $(i+1)^{th}$ agent leaves the convex hull). Intuitively, we can say that condition $\dot{\phi}_{i+1} < 0$ is very seldom verified, since agents, under the control law (5), tend to equalize the inter-agent distance (ρ_i), while ϕ_{i+1} tends to $2\pi/n$.

Even though we are still unable to prove if eventually all agents will stay permanently on the convex hull, simulation results appear to confirm such behavior. Fig. 7 shows a circle formation for $n = 20$ anonymous agents.

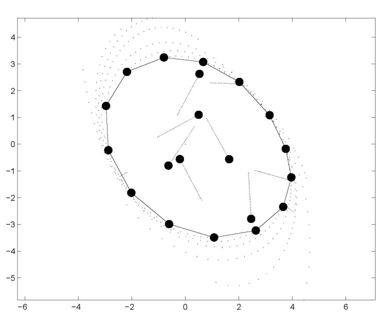

(a) $t = 3$

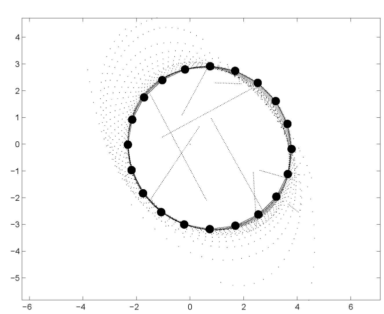

(b) $t = 20$

Fig. 7. Circle formation for $n = 20$ anonymous agents.

Now we show a critical case when $\dot{\phi}_{i+1} < 0$. Consider the formation of 8 agents in Fig. 8. For agents 2 and 6 we have:

$$\phi_{i+1} = 0; \qquad \dot{\phi}_{i+1} = \tfrac{5}{1}\sin(0-\alpha) + \tfrac{1}{5}\sin(\alpha) = -5\sin\alpha + \tfrac{1}{5}\sin\alpha \qquad i+1 = 2, 6. \tag{36}$$

If $\alpha = 0$ (rendez-vous formation), no agent leaves the convex hull; if, instead, $\alpha = \pi/8$ (circle formation), $\dot{\phi}_2 = \dot{\phi}_6 < 0$ and thus agents 2 and 6 leave the convex hull (see Fig. 8).

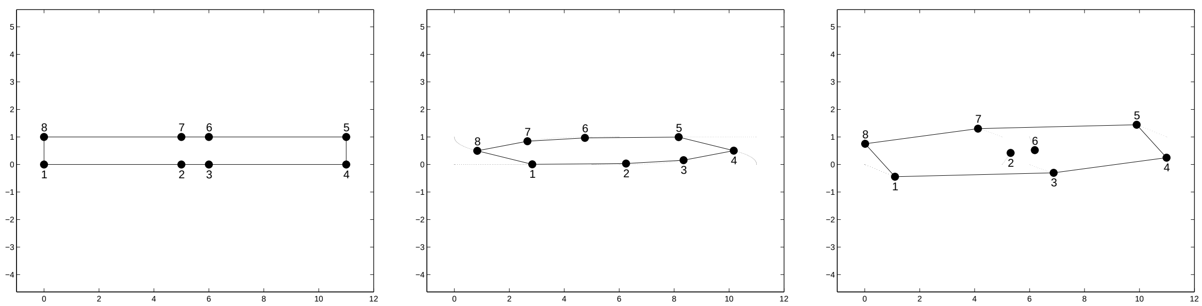

(a) Critical case: if $\alpha > 0$, $\dot{\phi}$ for agents 2 and 6 is negative while $\phi = 0$

(b) $\alpha = 0$: no agent leaves the convex hull

(c) $\alpha = \pi/8$: agents 2 and 6 leave the convex hull

Fig. 8. Critical case for the anonymous approach.

Remark 5.1: If $\alpha = 0$, when $\phi_{i+1} = 0$, $\dot{\phi}_{i+1}$ *can not* be negative and, thus, an agent on the convex hull will stay permanently on the convex hull. In other words, we have proved, as a particular case, that, under the classic cyclic pursuit control law, a convex polygon of pursuit stays convex.

VI. Application to coverage path planning

This section aims at illustrating how our generalized version of cyclic pursuit can be a suitable and advantageous approach for many problems currently of interest. We will show, without a detailed mathematical analysis, that it is possible to achieve more complicated geometric formations, by making the offset angle α a function of locally available information. In particular, we will study Archimedes spiral formations, since they are of interest in coverage path planning problems. Coverage path planning is critical in a variety of applications ranging from floor cleaning [19] to lawn mowing [20], mine hunting [21], harvesting [22], painting, etc. We will refer to the holonomic scenario; the extension to the non-holonomic scenario follows the same steps as in Section IV.

The objective of coverage path planning is to ensure that at least one agent eventually moves to within a given distance from any point in the target environment. Usually, each agent is assumed to be equipped with a device with a circular footprint of radius d; such a device can be either a sensing device (as in a search problem), an actuator (as in a lawn mowing problem), or a combination of both (as in a mine sweeping problem).

The design of coverage path planning algorithms raises several challenging issues, as coverage completeness, robustness, and coverage redundancy. Most available coverage algorithms rely either implicitly or explicitly on a cellular decomposition of the free space to complete the task. A cellular decomposition breaks down the target region into cells such that coverage in each cell is simple. Provably complete coverage is attained by ensuring the robot visits each cell in the decomposition [16]. One popular exact cellular decomposition technique, which can yield a complete coverage path solution, is the trapezoidal decomposition [23]. Since each cell is a trapezoid, coverage in each cell can easily be achieved with simple back and forth motions. Coverage of the environment is achieved by visiting each cell in the adjacency graph. An enhancement of trapezoidal decomposition is represented by the boustrophedon cellular decomposition [24], designed to minimize the number of excess lengthwise motions. Unfortunately, grid-map based algorithms require considerable memory, centralized off-line computation, and costly localization sensors (*e.g.*, GPS).

When considering a circular and obstacle-free environment, an alternative approach could be to consider n agents that move in an Archimedes spiral formation (an Archimedes spiral is a curve defined by a polar equation of the form: $\rho(\varphi) = a\varphi$). In fact, if the position of the center of the i^{th} agent's footprint follows the path defined by:

$$\rho_i(\varphi) = \frac{dn}{\pi}\,\varphi + \rho_0 - 2d\,(i-1), \tag{37}$$

the agents' footprints will cover any compact subset of the plane in finite time (provided the speed of advancement along such paths is bounded away from zero).

We are now going to show that n agents in cyclic pursuit, with an offset angle function of locally available information, are able to perform an Archimedes spiral formation. The resulting control policy will be static (*i.e.*, memoryless), decentralized, and will not rely on costly grid maps (unlike approaches based on cellular decomposition). Therefore, at least for a circular and obstacle-free environment, our version of cyclic pursuit provides an efficient way to solve the path planning problem. We mention that the rather strong assumption of a circular and obstacle-free environment nevertheless allows applicability to many practical problems like lawn mowing, automated farming, and mine sweeping of open areas.

A. Control policy for coverage path planning

Let us define a regular configuration as a configuration such that the centers of the agents' footprints $\boldsymbol{\xi}_i$, $i \in \{1,\dots,n\}$, are located on the vertices of a regular n-polygon. A system of n agents is in a regular configuration if and only if the following constraint is satisfied:

$$\boldsymbol{\xi}_{i+1} - \boldsymbol{\xi}_i = R[\theta_n(j-i)](\boldsymbol{\xi}_{j+1} - \boldsymbol{\xi}_j), \quad \forall i,j \in \{1,\dots,n\}, \tag{38}$$

where $\theta_n = 2\pi/n$.

Let the policy π_{spiral} be such that it assigns to the i-th agent the control input:

$$\boldsymbol{u}_i = R(\alpha_i)(\boldsymbol{\xi}_{i+1} - \boldsymbol{\xi}_i), \tag{39}$$

where:

$$\alpha_i = \frac{\pi}{n} + \arctan\left(\frac{2d}{\|\boldsymbol{\xi}_{i+1} - \boldsymbol{\xi}_i\|}\,\frac{\sin(\pi/n)}{\pi/n}\right). \tag{40}$$

Note that the computation of the control input for the i^{th} agent requires the knowledge of the relative position of the agent labelled by $i+1$ with respect to agent i. Thus, this control policy is *static* and *decentralized* and does not rely on costly grid maps.

Theorem 6.1: For any collection of $n \geq 2$ agents with dynamics described by (2) and control input (39)-(40), unconstrained workspace, and with initial conditions such that the agents are in a regular configuration and contained within a circle of radius d, the static feedback control policy π_{spiral} solves the path coverage problem for any bounded target set $\mathcal{Q}$.

Proof: First of all, we will show that the regular configuration constraint (38) is an invariant under the proposed policy. Assume that at time t_0 the agents are in a regular configuration. Let us write $r_i(t) = \boldsymbol{\xi}_{i+1}(t) - \boldsymbol{\xi}_i(t)$. Then, $\|r_i(t_0)\| = \bar{r}(t_0)$ and $\alpha_i(t_0) = \bar{\alpha}(t_0)$, for all $i \in \{1, \ldots, n\}$. The regular configuration constraint can be rewritten as $r_i - R[(j-i)\theta_n]r_j = 0, \quad \forall i, j \in \{1, \ldots, n\}$. Computing time derivative along system trajectories and considering that rotations about the same axis commute we get:

$$\frac{d}{dt}\left\{r_i - R[(j-i)\theta_n]r_j\right\} = R(\bar{\alpha})\left\{r_{i+1} - R[\theta(j-i)]r_{j+1} - r_i + R[\theta(j-i)]r_j\right\}.$$

Note that the above derivative is zero at all regular configurations; in other words, if the agents are in a regular configuration at a certain time instant, their differential evolution under the proposed policy is such that they remain in a regular configuration.

Furthermore, the centroid $\boldsymbol{\xi}_G = 1/n \sum_{i=1}^{n} \boldsymbol{\xi}_i$ of agents in regular configuration remains fixed; differentiating the position of the centroid, we get:

$$\frac{d}{dt}\boldsymbol{\xi}_G(t) = \frac{1}{n}\sum_{i=1}^{n} R(\bar{\alpha})r_i = \frac{1}{n}R(\bar{\alpha})\sum_{i=1}^{n} r_i = 0.$$

In the remainder of this proof, we will assume that $\boldsymbol{\xi}_G = 0$, without loss of generality, and indicate with $(\rho_i(t), \varphi_i(t))$ the polar coordinates with respect to $\boldsymbol{\xi}_G$ of the center of the i-th agent's footprint at time t.

In these coordinates we have $\dot{\rho}_i(t) = 2\rho_i(t)\sin(\bar{\alpha}(t) - \pi/n)\sin(\pi/n)$ and $\dot{\varphi}_i(t) = 2\cos(\bar{\alpha} - \pi/n)\sin(\pi/n)$. Eliminating time, we can write

$$\frac{d\,\rho_i}{d\varphi_i} = \rho_i(t)\frac{2d}{\bar{r}(t)}\frac{\sin\pi/n}{\pi/n},$$

integrating, and using the fact that in a regular configuration $\bar{r}(t) = 2\rho_i(t)\sin\pi/n$, we get

$$\rho_i = \frac{dn}{\pi}\varphi_i + c_i,$$

where the constants c_i depend on the initial conditions. Since at the initial time the agents were in a regular configuration contained in a circle of radius d, such constants can be found by setting

$$\frac{dn}{\pi}(\varphi_1 + \theta_n(i-1)) + c_i = \rho_0 \leq d.$$

Concluding, we get that the centers of the agents' footprints move along paths defined by equations of the form (37), *i.e.*, they move along Archimedes spirals, as desired.

Given any point in $\mathcal{Q}$ with polar coordinates (ρ_q, φ_q), it will always be possible to find $i \in \{1, \ldots, n\}$ in such a way that $|\rho_q - \rho_i(\phi_q)| \leq d$. In other words, since the agents move along their paths at non zero speed, such a point will be visited by one of the agents in finite time. ■

B. Discussion

Simulations suggest a very large region of attraction for agents starting off a regular configuration. Numerical simulation results about achieving Archimedes spiral trajectories with agents starting off a regular configuration are included in Fig. 9.

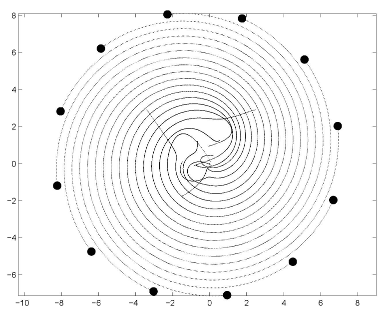

Fig. 9. Archimedes spiral trajectories for $n = 12$ agents with a footprint radius $d = 0.2$.

This approach is, intuitively, robust against agent losses, since when an agent disappears, say agent i, agent $i-1$ tends to cover, due to the nature of the control law, the past trajectory of agent i. Therefore, the approach may be suitable in hazardous applications as humanitarian demining. Numerical simulation for $n = 16$ agents that undergo 6 losses is provided in Fig. 10.

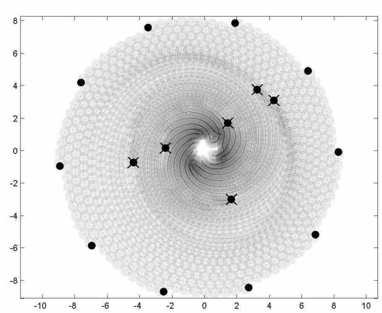

Fig. 10. Archimedes spiral trajectories for $n = 16$ agents that undergo 6 losses (agents with cross); the covered area is also shown.

VII. Conclusion

In this paper we have proposed a decentralized strategy aimed at achieving symmetric formations. It was shown that n agents, each one pursuing its leading neighbor along the line of sight rotated by a common offset angle, eventually converge to a single point, a circle or a logarithmic spiral pattern, depending on the value of the angle. The equilibrium formations are globally stable also when non-holonomic robots are considered.

Moreover, it was discussed a convex hull approach to make the agents totally anonymous and a possible application to coverage path planning.

There are many possible directions for future research, including (1) stability in presence of actuator saturation, (2) stabilization to a circle of desired radius by making the α angle dynamic, (3) convergence analysis of the Archimedes spiral formation; moreover, it could be interesting to study, as far as the anonymous approach is concerned, if eventually all agents stay permanently on the convex hull.

REFERENCES

[1] I. Suzuki, and M. Yamashita, *Distributed anonymous mobile robots: formation of geometric patterns*, Siam J. Comput., vol. 28, no. 4, pp. 13471363, 1999.

[2] E. W. Justh and P. S. Krishnaprasad, *Steering laws and continuum models for planar formations*, Proc. 42nd IEEE Conf. Decision and Control, Maui, HI, Dec. 2003, pp. 36093614.

[3] A. Jadbabaie, J. Lin and A. S. Morse, *Coordination of groups of mobile autonomous agents using nearest neighbor rules*, IEEE Trans. Automat. Contr., vol. 48, pp. 9881001, June 2003.

[4] T. Vicsek, A. Czirok, E. Ben Jacob, I. Cohen and O. Schochet, *Novel type of phase transitions in a system of self-driven particles*, Physical Review Letters, 75:12261229, 1995.

[5] J. Jeanne, N. E. Leonard and D. Paley, *Collective Motion of Ring-Coupled Planar Particles* To appear in Proc. 44th IEEE Conf. Decision and Control, 2005.

[6] D. Paley, N. E. Leonard and R. Sepulchre, *Oscillator Models and Collective Motion: Splay State Stabilization of Self-Propelled Particles*, To appear in Proc. 44th IEEE Conf. Decision and Control, 2005

[7] R. O. Saber and R. M. Murray, *Flocking with Obstacle Avoidance: Cooperation with Limited Communication in Mobile Networks*, Proc. of the 42nd IEEE Conference on Decision and Control, 2003.

[8] N. Leonard and E. Friorelli, *Virtual leaders, artificial potentials and coordinated control of groups*, Proc. 39th IEEE Conference on Decision and Control, Orlando, FL, 2001.

[9] Z. Lin, M. Broucke, and B. Francis, *Local control strategies for groups of mobile autonomous agents*, IEEE Trans. on Automatic Control, 49(4):622-629, 2004.

[10] J. A. Marshall, M. E. Broucke and B. A. Francis, *Formations of Vehicles in Cyclic Pursuit*, Ieee Transactions On Automatic Control, Vol. 49, No. 11, November 2004.

[11] J. A. Marshall, M. E. Broucke and B. A. Francis, *Pursuit Formations of Unicycles*, Automatica, vol. 41, no. 12, December 2005.

[12] A. M. Bruckstein, N. Cohen and A. Efrat, *Ants, crickets and frogs in cyclic pursuit*, Center Intell. Syst., Technion-Israel Inst. Technol., Haifa, Israel, Tech. Rep. 9105, 1991.

[13] B. d'Andra Novel, G. Campion, and G. Bastin, *Control of nonholonomic wheeled mobile robots by state feedback linearization*, Int. J. Robot. Res., vol. 14, pp. 543-559, 1995.

[14] J. R. T. Lawton, R. W. Beard and B. J. Young, *A Decentralized Approach to Formation Maneuvers*, IEEE Transactions On Automatic Control, Vol. 19, No. 6, pp. 933-941 December 2003.

[15] J. A. Marshall, *Coordinated autonomy: pursuit formations of multivehicle systems*, Ph.D. Thesis, 2005.

[16] H. Choset, *Coverage for robotics A survey of recent results*, Annals of Mathematics and Artificial Intelligence 31: 113126, 2001.

[17] P. J. Davis, *Circulant Matrices*, 2nd ed. New York: Chelsea, 1994.

[18] G. J. Tee, *Eigenvectors of compound-circulant and alternating circulant matrices*, Technical Report 479, University of Auckland, Department of Mathematics, 2002.

[19] J. Colegrave and A. Branch, *A case study of autonomous household vacuum cleaner*, AIAA/NASA CIRFFSS, 1994.

[20] Y. Y. Huang, Z. L. Cao and E. L. Hall, *Region filling operations for mobile robot using compuetr graphics*, Proc. of the IEEE Conference on Robotics and Automation, pp. 1607-1614, 1986.

[21] S. Land and H. Choset, *Coverage path planning for landmine location*, Third International Syposium on Technology and the Mine Problem, Monterey, CA, 1998.

[22] M. Ollis and A. Stentz, *First results in vision-based crop line tracking*, Proc. of the IEEE Conference on Robotics and Automation, 1996.

[23] J.C. Latombe, *Robot Motion Planning*, Kluwer Academic, Boston, MA, 1991.

[24] H. Choset and P. Pignon. *Coverage path planning: The boustrophedon decomposition*, Proceedings of the International Conference on Field and Service Robotics, Canberra, Australia, December 1997.